EFFECTS OF HUB ENDWALL GEOMETRY AND ROTOR LEADING EDGE SHAPE ON PERFORMANCE OF SUPERSONIC AXIAL IMPULSE TURBINE. PART I

M.V. Smirnov, A.A. Sebelev, N.A. Zabelin, N.I. Kuklina

Department "Turbines, Hydro machines and aero-engines"
Peter the Great St. Petersburg Polytechnic University (SPbPU)
St. Petersburg, Russia
e-mail: a.sebelev.turbo@mail.ru

ABSTRACT

The paper focuses on methods for an efficiency increasing of supersonic axial impulse turbines. There was chosen the axial turbine stage with axisymmetric nozzles and mean diameter 103.5 mm as the base model for a numerical and experimental investigation.

There were chosen two modifications of the base design to provide an efficiency increasing: modification of the rotor leading edge design and modification of the rotor hub endwall design.

The effect of these two factors on the turbine efficiency was analyzed separately. A preliminary numerical investigation showed that the rotor hub endwall modification provided an efficiency increasing up to 2% in comparison with the base model. Meanwhile, modification of the rotor leading edge shape did not provided significant efficiency increasing in comparison with the base model.

KEYWORDS

SMALL-SCALED TURBINES, SUPERSONIC TURBINES, ROTOR BLADE SWEEP, HUB ENDWALL CONTOURING

NOMENCLATURE

a_{th}	nozzle throat (mm)
B_2	blade wheel width (mm)
D_m	mean diameter (m)
G	mass flow rate (kg/s)
H_0	isentropic enthalpy drop (kJ/kg)
k	isentropic exponent
l_2	rotor blade height (mm)
n	rotational speed (rev/min)
p	pressure (MPa)
T	temperature (K)
r	radius coordinate (m)
x	length coordinate (m)
c	velocity in stationary frame (m/s)
w	velocity in relative frame (m/s)
φ, ψ	nozzle and blade wheel velocity ratios
α_1	nozzle outlet angle in stationary frame (deg.)
β_1	blade wheel inlet angle in relative frame (deg.)
β_2^*	blade wheel outlet angle in relative frame (deg.)
L	length (m)
M	Mach number
π	pressure ratio
u/C_0	stage specific speed
M_R	rotor torque (N·m)
Z	number of blades
ΔL	clearance value (mm)
ε	partial admission rate
η_{t-s}	total-to-static efficiency

Subscript

*	total parameter
ac	axial clearance
in	initial
tc	tip clearance
0	nozzle inlet
1	nozzle outlet
2	blade wheel outlet

INTRODUCTION

Pressure shocks appearance and unexpected flow separation regions are fundamental aerodynamic phenomena and the major source of comparably low supersonic stages efficiency (Natalevich (1979), Cho (2004), Klonowicz et al. (2014)).

Supersonic turbine stages for different purposes were widely investigated since 1955 up to nowadays. The earlier investigations were made mostly experimentally, while the latest studies are mostly computational. The advanced methods of characteristics are used to apply in case of supersonic vanes and rotor blades design, nevertheless, supersonic stage total-to-static efficiency tends to stay of about 0.4 – 0.5.

Tomas P. Moffitt (1958) studied a high-work stage for a rocket pump drive with an inlet rotor Mach number of 2 and aftermixing Mach number of 2.43. Divergent part of the nozzle was designed in accordance with supersonic design technics. A rotor design using the supersonic-vortex-flow theory was performed. A boundary layer thickness value was included to the design method. According to the experiments, the total-to-static stage efficiency (0.414) was significantly below the preliminary estimated value (0.504).

Louis J. Goldman (1972) performed a comparison of analytically predicted and experimentally obtained total-to-static stage efficiency values. The nozzle vanes and rotor blades design was performed in accordance with the method of characteristics for the isentropic flow of a perfect gas. Then the corrections were involved to the stage design, taking into account the displacement thickness. The nozzle vanes design was made in order to obtain aftermixing Mach number of 2.85 (Mach number in stationary frame at the rotor inlet). The actual value of total-to-static stage efficiency (0.39) was well below the preliminary estimated value (0.50). Author assumed that this was a consequence of an unexpected flow separation regions and laminar boundary layer losses.

Anderson et al. (1998) investigated a two stages super/transonic axial turbine for a pump drive in the framework of "Vulcan 2" project. A stage pressure ratio was equal to 12 in the design point. Due to non-optimal stage load coefficient the total-to-total efficiency remained rather low (0.4).

A supersonic single-stage axial turbine was numerically studied by Dorney et. al (2000). A pressure ratio was set as 5.33 for the investigated turbine. The method of characteristics was applied to design the nozzle. The nozzle outlet Mach number was found to be 1.46. Total-to-total and total-to-static efficiency reached 0.671 / 0.479 while the tip clearance as well as the rotating shroud was absent and 0.667 / 0.470 for the tip clearance of 2.5% span.

Investigations of a rotor blade shape effect on a performance of full-scale turbines show it to be prospective for an efficiency improvement. Wadia et al. (1998) investigated the effect of the rotor blades sweep on the efficiency of a compressor first stage of an aircraft gas turbine. There was obtained an efficiency increasing up to 0.44% in case of supersonic flow regime with using backward blade sweep. Pullan and Harvey (2008) and Yoon et al. (2014) achieved the same results for axial flow turbines.

Jeong et al. (2015) numerically investigated the impact of a rotor blade sweep on the performance of a small-scaled supersonic impulse turbine. Backward sweep (+15°) and forward sweep (-15°) of the rotor blade were investigated. It was shown that backward sweep provided up to 1% efficiency increasing in comparison with the base model. Meanwhile, forward sweep of the rotor blade provided 0.6% efficiency decreasing in comparison with the base model.

A hub endwall contouring effect on secondary losses was widely investigated for full-scale turbines. Hartland et al. (2000) investigated a hub endwall contouring effect on total pressure losses in a blade wheel of an axial flow turbine. Total pressure losses were decreased by 15.3% with implementation of the hub contouring. Harvey et al. (2002) investigated an influence of hub contouring on the efficiency of an axial flow turbine. An efficiency improvement obtained was about 1.8% at the design point.

Dorney et al. (2002) investigated the effects of endwall optimization and blade stacking on a stage efficiency. A pressure ratio was set as 8.81. Due to high total inlet temperature (1236 K), the nozzle outlet flow reached Mach number of 1.15-1.37. Four models were studied in the research:

the original stage design, two stages with modified endwall and the stage with vanes, re-stacked along the radial line connecting the trailing edge points. They pointed out that endwall optimization may decrease as well as increase the stage efficiency. Blade re-stacking resulted in the considerable increasing of the stage efficiency due to decreasing the separation flow region. Total-to-static efficiency reached 0.553 / 0.568 for the basic stage design and endwall-optimized design. Re-stacked airfoil showed total-to-static efficiency of 0.618.

Akin et al. (2015) used an adjoint method and RANS simulation for optimal hub endwall contouring. Maximum polytrophic efficiency was a function of the optimization process. As a result of the optimization the polytrophic efficiency of a low pressure stage increased by 6.2% and the hub separation was totally suppressed.

Based on the studies presented above, classical design approach can't provide total-to-static efficiency higher than 0.4 – 0.5. A rotor blade sweep as well as hub endwall contouring was shown to strongly affect supersonic turbines efficiency. Thus, these approaches seem to be a key for further efficiency improvement. Furthermore, the additive technologies as 3D printing discard technological restrictions and allow realizing practically new stage design.

The scope of the current paper is to investigate a new design of a small-scaled supersonic axial flow turbine based on the principles of rotor blade sweep and hub endwall contouring. The basic and modified stage design and numerical efficiency evaluation are presented in this paper (Part I). An experimental investigation of the 3D-prototyped polyamide stages are going to be presented in Part II.

INVESTIGATION OBJECT

The Turbine Design

Three types of supersonic stage design were considered:

- ST-26 – a stage with straight centralized nozzles, the nozzle outlet and rotor blades inlet are planar and normal to the stage rotation axis.
- ST-26A – the modified stage ST-26 with the rotor blades backward sweep. The nozzle outlet and rotor blades inlet are non-planar.
- ST-26B – the modified stage ST-26A with the hub endwall modification (smoothly transitioned hub overlap).

The details of the stages geometry are presented in table 1.

Table 1: Design parameters of the stages ST-26, ST-26A, ST-26B

Parameter	Dimensions	Value ST-26	Value ST-26A	Value ST-26B	Parameter	Dimensions	Value ST-26	Value ST-26A	Value ST-26B
Throat shape	-	Circular			Z_1	-	12		
D_m	mm	103.5			$\beta_1 = \beta_2$*	deg.	36		
ε	-	0.576			Z_2	-	55		
a_{th}	mm	5.08			l_2	mm	10		
α_1	deg.	20.00			B_2	mm	9.5	12	12
ΔL_{ac}	mm	1.0			Hub transition	mm	Step-type		Smooth
ΔL_{tc}	mm	0.5							

ST-26 – supersonic stage with straight centralized nozzles

The nozzle of the stage ST-26 is presented by the straight axisymmetric convergent-divergent channel. A Laval nozzle design is required due to a high pressure ratio of π = 2.67 and high estimated Mach number (M > 1.3). A relative Mach number at the rotor inlet is expected to be transonic.

A subsonic part of the nozzle is designed according to a Vitoshinski equation which is usually used for a conjugating of two tubes with different diameters (Dejch (1970)):

$$r = \frac{a_{th}}{\sqrt{1-\left[1-\left(\frac{a_{th}}{r_{in}}\right)^2\right]\cdot\frac{\left(1-\frac{3x^2}{L^2}\right)^2}{\left(1+\frac{x^2}{L^2}\right)^3}}}. \quad (1)$$

The nozzle throat is circular. A supersonic part of the nozzle is a divergent axisymmetric channel. The rotor of the ST-26 stage is shrouded. The flow path of the ST-26 stage is presented in figures 1a, 2a.

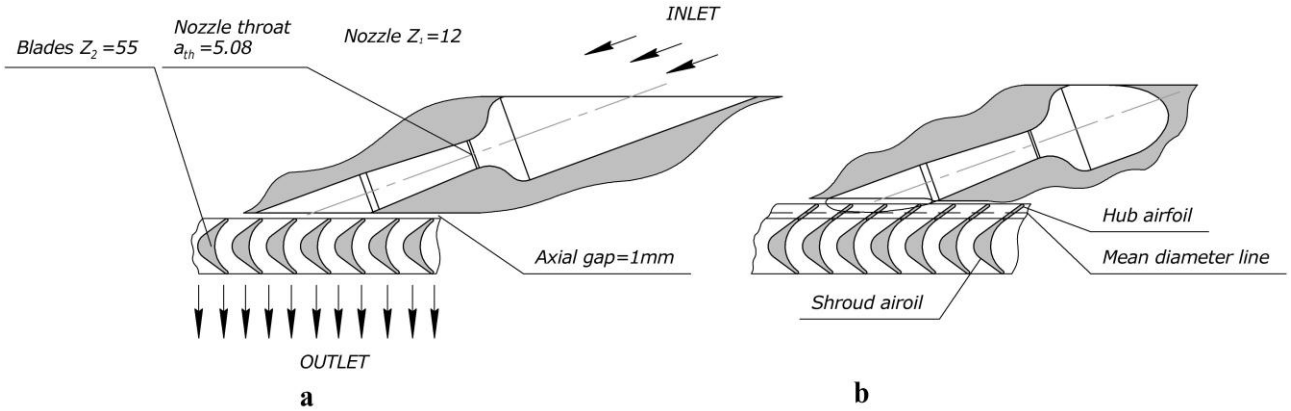

Figure 1: Blade-to-blade view of the ST-26 (a) and ST-26A (b) stages

ST-26A – stage with straight centralized nozzles and rotor blades backward sweep

Pressure shocks and rotor-stator interaction are the most significant sources of losses in supersonic turbine stages. While the rotor-stator interaction surface is normal to the stage rotation axis, all the interaction in the spanwise direction occurs in this plane. On the one hand, this leads to the strong system of the shock waves by itself. On the other hand, this precipitates a rising of secondary losses due to high flow instability in hub region. The reduction of the shock losses with using rotor blades sweep was predicted by Denton (1998).

The modification of the basic stage aimed to provide the following:

1) decreasing of the secondary losses in the hub region with using the rotor blades backward sweep at the first 50% of span;
2) arranging the rotor-stator interaction into the surface with larger area in order to make the shock system weaker. On this account, the interaction plane needs to be turned to some angle with respect to axial direction at the second 50% of span.

The subcritical part of the nozzle, throat and the divergent part have the same design as for the stage ST-26. The divergent part of the nozzle is axially cut at 2.5 mm at the hub and 0 mm at the shroud. Oppositely, the extension of the rotor blade leading edge is 0 mm at the shroud and 2.5 mm at the hub. The axial gap is 1 mm in axial direction (differs in normal direction). These modifications are presented in figures 1b, 2b.

ST-26B – stage with straight centralized nozzles, rotor blades backward sweep and smoothly transitioned hub overlap

An endwall design affects the flow due to the interaction of a hub vortex and the flow core, resulted in the increasing of secondary losses. In order to improve the hub flow structure, special hub design was proposed in ST-26B stage. The nozzle and rotor blades have the same design as for ST-26A stage, including axial the rotor blades sweep. A smooth transition is applied to improve the

hub overlap. The ST-26B meridional contour is presented in figure 2c. 3D design of the stages is shown in figures 2, 3.

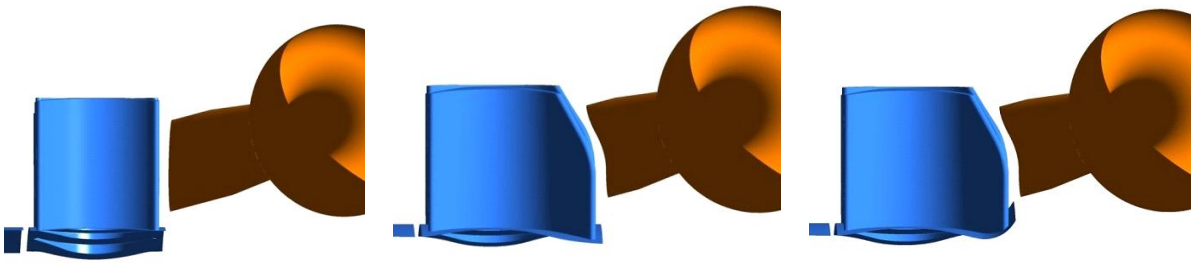

a **b** **c**

Figure 2: Comparison of the three design types – ST-26 (a), ST-26A (b), ST-26B (c) (shroud is hidden)

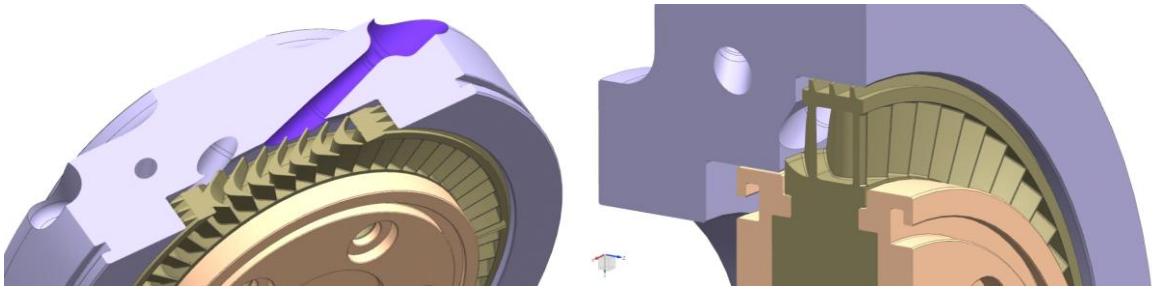

Figure 3: 3D details of the ST-26B stage design

Initial Conditions

The basic turbine stage is designed for the pressure recovery turbogenerator for a gas-distribution plant and operates with methane. The main operating conditions of the basic turbine stage are presented in table 2.

The testing of the basic and modified turbine stages is going to be performed in the SPbPU "cold-flow" air test rig. The choice of the test conditions is based upon the similarity rules as described by Kirillov (1972) and Traupel (1977). In case of an impulse axial flow turbine the same flow kinematics and the same stage efficiency can be provided with using the same specific speed u/C_0 according to the Banki equation:

$$\eta_u = 2\varphi \frac{u}{C_0}\left(\cos\alpha_1 - \frac{u}{C_0}\right)\cdot(1+\psi). \qquad (2)$$

This statement holds for the equal φ and ψ ratios. It is evident that flow regime affects the φ and ψ ratios. Thus, it is necessary to obtain the same Mach and Reynolds numbers to achieve the same stage parameters in the air-flow experiment. The nozzle outlet isentropic Mach number could be obtained with using the following equation:

$$M_{1t} = \sqrt{\frac{2\cdot\left(1-\pi^{\frac{1-k}{k}}\right)}{(k-1)\cdot\pi^{\frac{1-k}{k}}}}. \qquad (3)$$

Analysis of the equation (3) in case of methane and air shows that a very close M_{1t} values could be obtained with using the same pressure ratios π. Reynolds numbers at the nozzle outlet in this case are in self-similarity region as represented in table 2.

The turbine outlet pressure was chosen with regard to the pressure losses in the test rig exhaust system. The turbine inlet temperature was chosen so as to provide safe operation of the plastic blade wheel in the whole operation range. The chosen initial conditions for air testing are presented in table 2.

Table 2: Initial parameters of the methane- and air-operated turbine stage

Parameter	Dimensions	Methane-operated stage	Air-operated stage
p_0^*	MPa	0.400	0.272
T_0^*	K	288.0	320.0
p_2	MPa	0.150	0.102
π	-	2.67	
k	-	1.311	1.400
H_0	kJ/kg	129.4	78.5
u/C_0	-	0.40	
n	rev/min	45000	32000
M_{1t}	-	1.298	1.272
Re_1	-	$5.12 \cdot 10^5$	$2.53 \cdot 10^5$

NUMERICAL ANALYSIS

Numerical Simulation Method

ANSYS CFX was used to provide the numerical simulation. The original relation between the number of nozzles and rotor blades is 12 / 5. The relation 1 / 5 and periodic boundary conditions were used in the computational model. The modeling of the blade wheel tip clearance was also considered in the numerical model. Total parameters at the inlet (p_0^* = 0.272 MPa, T_0^* = 320 K) and static pressure at the outlet (p_2 = 0.102 MPa) were specified as boundary conditions in the computational model.

There was used a high-Reynolds version of the k-ω SST turbulence model described by Menter (1994). The parameters of the computational domains discretization were chosen on the base of the grid independency study, presented by Zabelin et al. (2013). The grid sizes are: 3.23 million of nodes for 1 nozzle sector and 1.42 million of nodes for 1 blade wheel sector. The total grid size varies from 10.34 to 12.32 million of nodes for different stages. Maximum values of y^+ parameter were 44 for the stator parts and 38 for the rotor parts. The limitations of this approach, described by Dorney et al. (1999) and Denton (2010), were taken into account. In particular, the stage efficiency evaluation was based on the rotor blades torque. The direct flow enthalpy method was not considered.

Transient rotor-stator interaction was taking into account by performing URANS simulations. The time step was evaluated as $2.579 \cdot 10^{-6}$ s. The full transient simulations were performed in order to obtain averaged values of the mass flow rate and blade wheel torque. Steady-state solutions were used as initial conditions for URANS simulations.

Monitoring of the RMS residuals, imbalances and turbine efficiency and power output were used to control the convergence of a steady-state solution process. The convergence criteria for the steady-state solutions were:

- drop of the RMS residuals more than 10^2;
- imbalances less than 0.5%;
- fluctuation of the turbine efficiency and power output less than 5%.

The total-to-static stage efficiency was calculated with using the following equation:

$$\eta_{t-s} = \frac{M_R \cdot \pi \cdot n}{30 \cdot G \cdot H_0}. \qquad (4)$$

The $\eta_{t-s} = f\,(u/C_0)$ curve was obtained using the linear character of the $M_R = f\,(u/C_0)$ function, as described by Kirillov (1972) and Traupel (1977).

Discussion of the Results

ST-26

As shown in figure 4 the first oblique shock wave in the nozzle has a conic shape. It reflects from the nozzle wall and then takes part in the formation of the complex shock waves system together with the shock waves formatted on the nozzle trailing edge. These complex phenomena lead to additional losses of kinetic energy in the nozzle oblique cut.

Analysis of the flow structure in the nozzle oblique cut shows an occurrence of highly detached flow regions. The possible reason of such a phenomenon is the part-load stage conditions due to incorrect scaling between methane and air. It could be clearly seen that the flow in the relative frame is totally subsonic except the small leading edge regions with negative incidence.

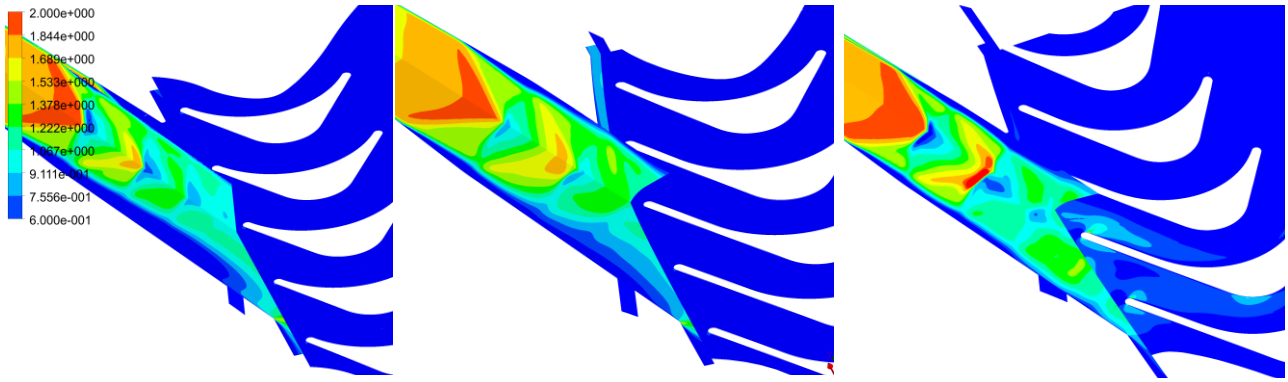

a **b** **c**

Figure 4: Transient averaged Mach number fields at the stages – ST-26 (a), ST-26A (b), ST-26B (c)

The interaction between the high-speed and low-speed flows leads to appearance of the spurious vortices at the blade wheel inlet as illustrated in figure 5. It can be seen that approximately one half of the blade wheel inlet sector is occupied by the low-speed flow.

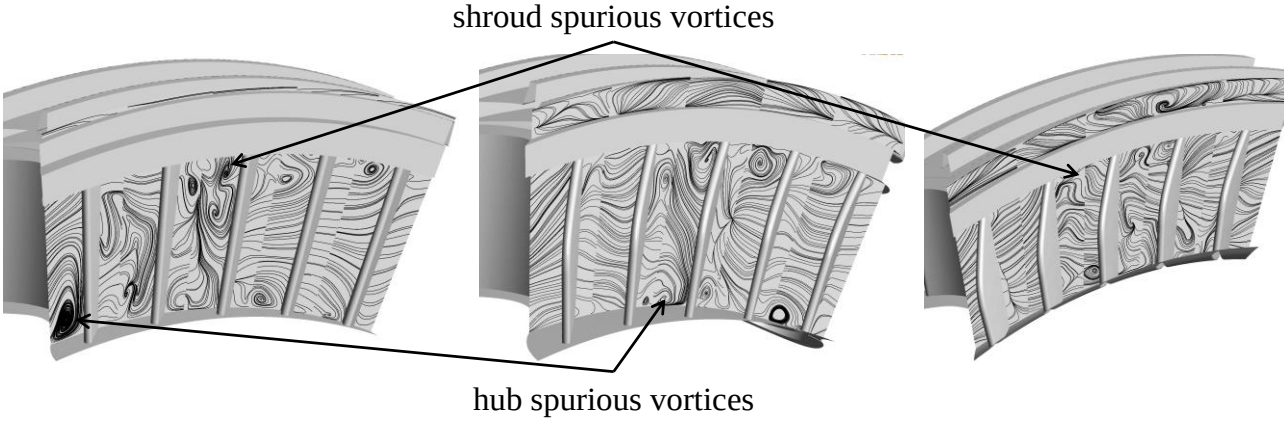

a **b** **c**

Figure 5: The flow structure at the blade wheel inlet – ST-26 (a), ST-26A (b), ST-26B (c)

ST-26A

Analysis of the flow structures at the ST-26 and ST-26A nozzles oblique cuts shows that in case of the ST-26A stage the separated flow regions becomes smaller. Evaluation of the blade wheel inlet and outlet pressures shows that in case of the ST-26A stage the nozzle pressure ratio becomes higher (see table 3). The only reason for such a phenomenon is the different design of the blade wheels. While the nozzle outlet flow is fully supersonic in the direction of the c_1 velocity it is still subsonic in the axial direction and may affect the nozzle outlet flow. This phenomenon was experimentally visualized by Cho et al. (2004) and is represented in figure 6 in terms of axial Mach number.

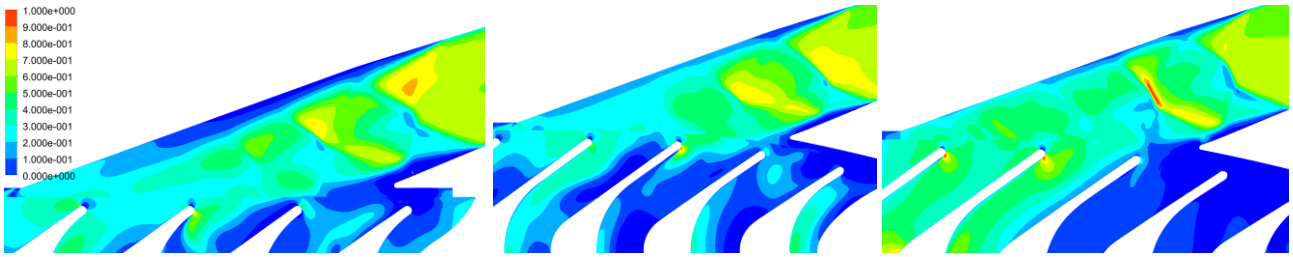

a **b** **c**

Figure 6: Axial Mach number fields at the relative frame (mean diameter) – ST-26 (a), ST-26A (b), ST-26B (c)

Table 3. Pressure conditions of the ST-26, ST-26A and ST-26B blade wheels

	ST-26	**ST-26A**	**ST-26B**
p_1, Pa	94164	92454	90537
p_2, Pa	100796	100543	100374

Analysis of the flow structure at the mean diameters shows that the leading edge backward sweep is helpful for stabilizing the flow at the blade wheel inlet (see figure 7). This positively affects the flow structure at the blade wheel inlet and leads to minimizing of the spurious vortices sizes as shown in figure 5. It must be emphasized that in case of the leading edge backward sweep only 25% of the rotor blades has the negative incidence angles as can be seen in figure 7.

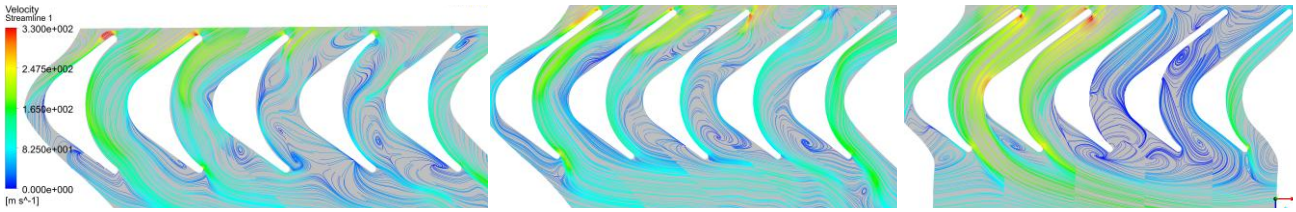

a **b** **c**

Figure 7: The flow structure at the mean diameter – ST-26 (a), ST-26A (b), ST-26B (c)

ST-26B

Analysis of the flow structures at the ST-26A and ST-26B nozzles oblique cuts shows that in case of the ST-26B the detached flow regions are nearly to be suppressed. The ST-26B nozzle pressure ratio is higher than in case of the ST-26A (see figure 4). Analysis of the flow structures at ST-26A and ST-26B blade wheels inlets have not showed up significant differences (see figure 5). However, the only reason for an efficiency increasing in case of ST-26B is smoothed design of the hub endwall. This design aimed at decreasing of the negative influence of the step-type hub overlap on the spurious hub vortex formation.

Analysis of figure 5 shows that the hub spurious vortex has lower size and intensity in case of ST-26B turbine stage. As a consequence the mixing losses through the high-speed and low-speed flows interaction are lower in case of ST-26B. Physically, it means that a hydraulic resistance of the ST-26B blade wheel is lower because of the minimizing of the hub spurious vortex (see table 3). As it can be seen in table 3, the ST-26A and ST-26B blade wheels have diffuser behavior due to strongly oversized flow path. This aspect has to be improved in further modification.

Evaluation of the stages performance

Numerically obtained efficiency of the ST-26, ST-26A, ST-26B stages is below its common values for traditional supersonic stages. The total-to-static efficiency of the ST-26 stage is estimated as 0.455. The total-to-static efficiency of the ST-26A and ST-26B stages is 0.435 and 0.455 respectively. The possible reason of such a result is the part-load stage operation due to incorrect scaling between methane and air. In this case the backward sweep of the rotor leading edge provides higher ventilation losses which leads to the efficiency drop down in the modified stage. However, the positive effect of the hub contouring provides 2% efficiency increasing in the ST-26B stage compared to the ST-26A stage. This result allows expecting of the same or higher efficiency increasing at the design point. The experimental investigations of the abovementioned stages will clarify the obtained results and are going to be presented in the next part of the present paper.

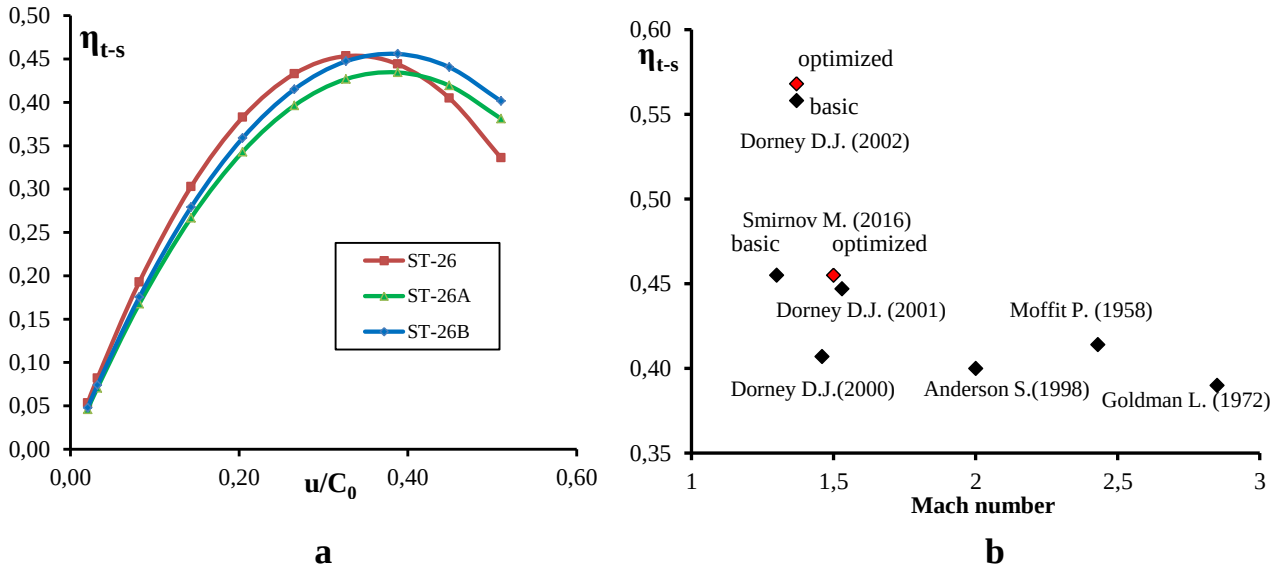

Figure 8: Total-to-static efficiency of the investigated stages (a) and its comparison with the overview of supersonic stages efficiency

CONCLUSIONS

The scope of the present research was the numerical investigation of the supersonic axial turbine stages with straight centerline nozzles. The Maximum Mach number at the nozzle outlet was 1.5. The boundary layer separation in the nozzle oblique cut and its interaction with an oblique shock wave were established. The details of the spurious vortices formation at the blade wheel inlet were described and analyzed. It was shown that formation of these vortices leads to the high losses of the flow kinetic energy through its dissipation.

There were proposed two modification of the basic stage (ST-26): the backward sweep of the rotor blade leading edge and the hub endwall contouring. The modification of the leading edge shape provided the efficiency decreasing due to the stage part-load operation. Somehow, the flow uniformity was significantly improved because of a stabilizing of the flow in hub region and reorganization of the shock system. The hub endwall contouring resulted in 2% of total-to-static efficiency increasing compared to the first modification and provided the same efficiency as the basic stage.

ACKNOWLEDGEMENTS

The author crew would like to thank the Russian Ministry of Education for funding (grant No.14.578.21.0127) and the colleagues from STC "Microturbine Technology" for the technological support of the project.

REFERENCES

Akin, M.B., Pieringer, P., Sanz, W., (2015), *Optimization of a low pressure turbine stage by hub endwall contouring of the mid turbine frame using an adjoint method*. Proceedings of the 12th International Symposium on Experimental Computational Aerothermodynamics of Internal Flows, Lerici, Italy. ISAIF12-029.

Andersson, S., Lindeblad, M., Wahlen, U., (1998), *Performance test results for the Vulcain 2 supersonic / transonic turbine*. AIAA Paper: AIAA/ASME/SAE/ASEE Joint Propulsion Conference and Exhibit. No. 98-3999.

Cho, J.-J., Jeong, S.-I., Kim, K.-S., Lee, E.-S., (2004), *An experimental study on the flow characteristics of a supersonic turbine cascade as pressure ratio*. KSAS International Journal, Vol. 5, No. 2, pp. 9 – 17.

Dejch, M.E., (1970), *Gazodinamika diffuzorov i vyhlopnyh patrubkov turbomashin*. Jenergija, Moscow, 384 p.

Denton, J.D., Xu, L., (1998), *The exploitation of three-dimensional flow in turbomachinery design*. Proc. IMechE Part C: Journal of Mechanical Engineering Science, Vol. 213, No. 2, pp. 125 – 137.

Denton, J., (2010), *Some limitations of turbomachinery CFD*. Proceedings of the ASME Turbo Expo 2010: Power for Land, Sea and Air, Glasgow, UK. GT2010-22540.

Dorney, D.J., Griffin, L.W., Huber, F.W., Sondak, D.L., (2002), *Effects of endwall geometry and stacking on two-stage supersonic turbine performance*. Proceedings of the 40th AIAA Aerospace Sciences Meeting and Exhibit, Reno, NV, USA. AIAA-2002-78.

Dorney, D.J., Griffin, L.W., Huber, F.W., Sondak, D.L., (2001), *Unsteady flow in a supersonic turbine with variable specific heats*. Journal of Propulsion and Power, Vol. 18, No. 2, pp. 493 – 496.

Dorney, D.J., Griffin, L.W., Huber, F.W., (2000), *A Study of the effects of tip clearance in a supersonic turbine*. Journal of Turbomachinery, Vol. 122, pp.674 – 683.

Dorney, D.J, Griffin, L.W., Gundy-Burlet, K.L., (1999), *Simulations of the flow in supersonic turbines with straight centerline nozzles*. Journal of Propulsion and Power, Vol. 16, pp. 370-375.

Goldman, L.J., (1972), *Supersonic turbine design and performance*. TM X-67961, NASA, Cleveland, Ohio.

Hartland, J.C., Gregory-Smith, D.G., Harvey, N.W., Rose, M.G., (2000), *Nonaxisymmetric turbine end wall design: Part II – Experimental validation*. Journal of Turbomachinery, Vol. 122, No. 2, pp. 286 – 293.

Harvey, N.W., Brennan, G., Newman, D.A., Rose, M.G., (2002), *Improving turbine efficiency using non-axisymmetric end walls: validation in the multi-row environment and with low aspect ratio blading*. Proceedings of ASME Turbo Expo 2002, Amsterdam, The Netherlands. GT-2002-30337.

Jeong, S., Choi, B., Kim, K., (2015), *Rotor blade sweep effect on the performance of a small axial supersonic impulse turbine*. International Journal of Aeronautical & Space Science, Vol. 16, No. 4, pp. 571 – 580.

Kirillov, I.I., (1972), *Teorija turbomashin*. Mashinostroyenie, Leningrad, 533p.

Klonowicz, P., Hereble, F., Preißinger, M. and Brüggemann D., (2014), *Significance of loss correlations in performance prediction of small scale, highly loaded turbine stages working in Organic Rankine Cycles*. Energy, Vol. 72, pp. 322 – 330.

Menter, F. R., (1994), *Two-Equation eddy-viscosity turbulence models for engineering applications*. AIAA Journal, Vol. 32, No. 8, pp. 1598 – 1605.

Moffit, T.P., (1958), *Design and experimental investigation of a single-stage turbine with a rotor entering relative Mach number of 2*. RM E58F20a, NACA, Cleveland, Ohio.

Natalevich, A.S., (1979), *Vozdushnye mikroturbiny*. Mashinostroyenie, Moscow, 192p.

Pullan, G., Harvey, N.W., (2008), *The influence of sweep on axial flow turbine aerodynamics in the endwall region*. Journal of Turbomachinery, Vol. 130, No. 4, Paper No. 041011.

Traupel, W., (1977), *Thermische Turbomaschinen*. 3. Aufl., Springer, Berlin, 579p.

Wadia, A.R., Szucs, P.N., Crall, D.W., (1998), *Inner workings of aerodynamic sweep*. Journal of Turbomachinery, Vol. 120, No. 4, pp. 671 – 682.

Yoon, S., Denton, J., Curtis, E., Longley, J., Pullan, G., (2014), *Improving intermediate pressure turbine performance by using a nonorthogonal stator*. Journal of Turbomachinery, Vol. 136, No. 2, Paper No. 021012.

Zabelin, N.A., Rakov, G.L., Rassokhin, V.A., Sebelev, A.A., Smirnov, M.V., (2013), *Investigation of fluid flow highlights in low flow-rated LPI turbine stages*. St. Petersburg State Polytechnical University Journal, Vol. 166, No. 1, pp. 45 – 53.